12

Morphometric analysis of cranial morphology in pinnipeds (Mammalia, Carnivora): convergence, ecology, ontogeny, and dimorphism

KATRINA E. JONES AND ANJALI GOSWAMI

Introduction

Pinnipeds are a clade of secondarily aquatic arctoid carnivorans, including 34 extant species dispersed across most of the world's oceans. Extant species are separated into three families (Figure 12.1): Odobenidae (walruses, 1 species), Phocidae (seals, 19 species), and Otariidae (sea lions and fur seals, 14 species) and display a wide range of ecological diversity (Reeves *et al.*, 2002). Predominantly, pinnipeds are generalist feeders. They are opportunistic, and their diets may vary annually, between colonies and between individuals within a colony (King, 1983; Sinclair and Zeppelin, 2002; Williams *et al.*, 2007). However, several species have evolved more specialist feeding techniques: (1) *Odobenus rosmarus* is a suction feeder, using powerful facial musculature to produce forces large enough to extract molluscs from their shells (Adam and Berta, 2002); *Erignathus barbatus* (Phocidae) also uses suction feeding (King, 1983; Marshall *et al.*, 2008); (2) *Lobodon carcinophagus* (Phocidae) is a filter feeder; it uses multicuspidate teeth to sieve out krill as water is expelled from the mouth; (3) *Hyrdrurga leptonyx* (Phocidae) feeds on large, warm-blooded prey such as penguins and seal pups (Adam and Berta, 2002).

Reproductive strategies of the pinnipeds are also diverse. Otariids are universally dimorphic with large harems. Their young are weaned over long periods of up to 2 years whilst learning to forage (Kovacs and Lavigne, 1992; Schulz and Bowen, 2004). On the other hand, phocid young are relatively precocial (4–50 days weaning) and learn foraging skills after leaving their mothers. Phocids also show a diversity of mating strategies and degree of dimorphism (Schulz and Bowen, 2004). It has been hypothesised that this shorter time spent on land has allowed phocids to exploit a broader range of

Carnivoran Evolution: New Views on Phylogeny, Form, and Function, ed. A. Goswami and A. Friscia. Published by Cambridge University Press.

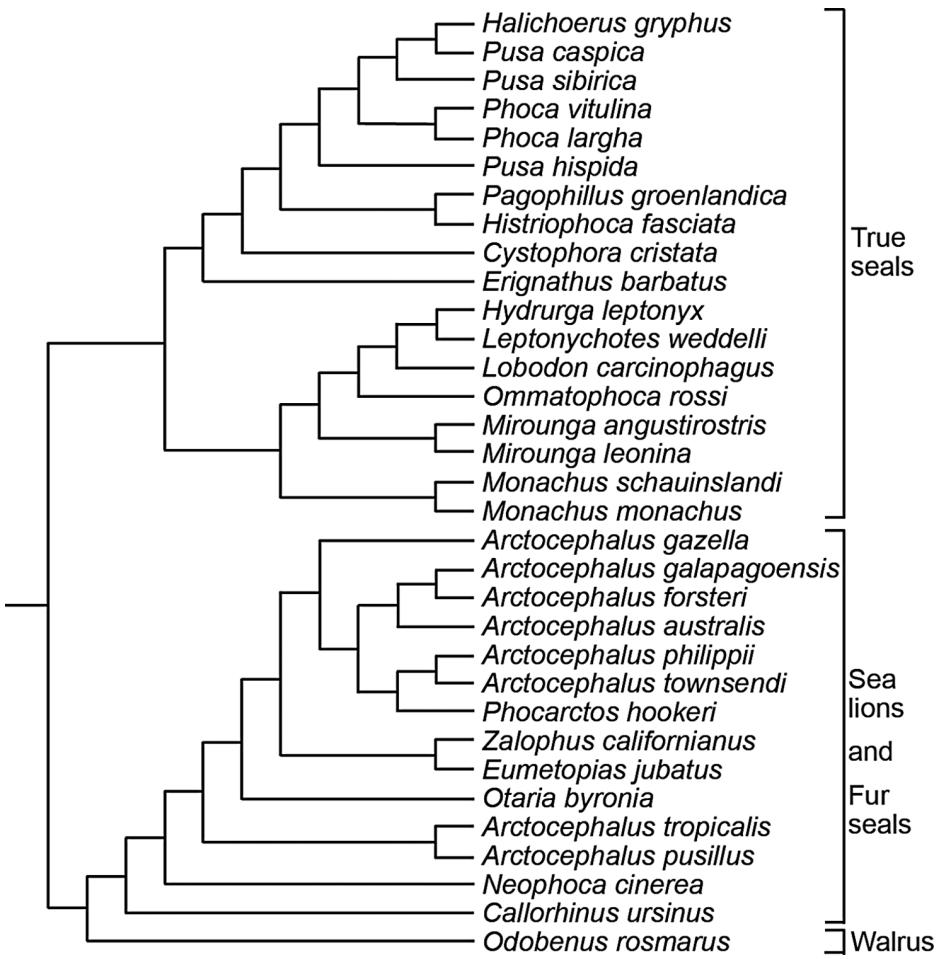

Figure 12.1 Composite phylogeny for extant pinnipeds (Wynen *et al.*, 2001; Arnason *et al.*, 2006).

habitats, including polar regions (Kovacs and Lavigne, 1992; Schulz and Bowen, 2005). Odobenids show extremely long lactation times of three years. During this period, young walruses often accompany mothers on foraging trips.

Despite these many interesting ecological differences, research into pinniped morphology has been fairly limited, and pinnipeds have received much less attention than other marine mammals, such as cetaceans and sirenians. Most research on pinnipeds has focused on taxonomy and phylogenetic relationships, which have been subject to much disagreement. Molecular work (Flynn *et al.*, 2005, this volume; Arnason *et al.*, 2006) suggests a closer relation between otariids and odobenids (forming the Otaroidea clade). Conversely,

morphology-based work (Adam and Berta, 2002; Deméré *et al.*, 2003) suggests a closer link between phocids and odobenids (Phocomorpha Clade). The relationship of pinnipeds to other carnivorans has also been contentious, with some morphological studies divided between a closer relationship of Pinnipedia to either Ursidae (Adam and Berta, 2002; Arnason *et al.*, 2006) or Musteloidea (Sato *et al.*, 2006). The latter relationship is also supported by recent molecular analyses across all Carnivora (Flynn *et al.*, 2005).

Perhaps because of early controversies in pinniped relationships, particularly pinniped monophyly (Wyss, 1988), several studies have focused on identifying traits that define pinnipeds. Surprisingly, comparative studies of various traits across Carnivora have indicated that many ecological, life-history and morphological factors fail to discriminate between pinnipeds and a paraphyletic grouping of terrestrial carnivorans (fissipeds; Bininda-Edmonds and Gittleman, 2000; Bininda-Edmonds *et al.*, 2001). Aquatic adaptations found to define pinnipeds were a larger brain size for perception in a 3D environment and longer head and body sizes for a more hydrodynamic form. Smaller litter sizes and shorter interbirth times in pinnipeds were also indicative of a more k-adapted reproductive strategy.

Pinnipeds are first known from late Oligocene (27–25 Mya) fossils of *Enaliarctos mealsi* from the Pacific coast of North America (Berta *et al.*, 1989), although a recently discovered early Miocene pinniped from the Canadian Arctic may represent a more transitional form with webbed feet, rather than flippers like *Enaliarctos* (Rybczynski *et al.*, 2009). The Otarioidea/Phocidae split is placed at around 33 Mya using molecular clock dating, predating the earliest fossils by 5 Mya (Arnason *et al.*, 2006). The Odobenidae/Otariidae divergence was placed at 27 Mya, though the oldest fossils (odobenids) are middle Miocene, ~14 Mya old (Arnason *et al.*, 2006). The earliest otariid fossils are found in the late Miocene, although the first unambiguous crown otariids do not appear until the late Pliocene (Deméré *et al.*, 2003). The basal extant phocid split of monachine and phocine phocids is placed in the early Miocene, ~22 Mya, by molecular estimates, and the oldest fossils that can be clearly assigned to one of these two subclades are late early Miocene (Arnason *et al.*, 2006). The phocid crown group is much older and includes more extinct species than that of crown otariids or crown odobenids, both of which are characterised by more stem taxa.

Many of the studies of early pinniped evolution have focused on paleobiogeography (Muizon, 1982; Deméré *et al.*, 2003), with several events potentially having a vicariant effect on pinniped evolution. For example, early pinniped divergences have been related to the growth of ice during late Oligocene glaciations, which may have caused increased coastal upwelling and ocean stratification. During the Pliocene, the closure of the Isthmus of Panama shut

off an east–west dispersal corridor and caused isolation of Pacific and Atlantic pinnipeds, leading to speciation. Further, the adaptation of phocines to cold waters in the Pleistocene caused a high-latitude radiation. This was compounded by glacioeustatic oscillations that acted to isolate colonies and cause more speciation. These examples, and many others, suggest that changing climate and circulation patterns have had a great effect on the evolution of pinnipeds (Deméré *et al.*, 2003).

Fewer studies have focused on the morphological evolution of pinnipeds. Early work (Repenning, 1976), based on observation and qualitative analysis of morphology, noted the importance of adaptive evolution towards a marine lifestyle reflected in fossil and extant forms and the variation in these features between the three extant families. Later, more quantitative methods were used with discrete features (Adam and Berta, 2002), to more accurately link prey capture strategies with anatomy, separating the clade into four groups based on ecology and morphology: pierce feeders, suction feeders, filter feeders, and grip-and-tear feeders.

Studies quantitatively examining morphological diversity of pinnipeds are very limited. A series of 2D traditional morphometric analyses of the cranium in otariid species and subspecies were conducted to examine otariid taxonomy and geographic variation (Brunner, 1998, 2003; Brunner *et al.*, 2002). Another recent investigation used 2D geometric morphometric analyses of the ventral view of the cranium to study the development of dimorphic features in three otariid species: *Arctocephalus australis*, *Callorhinus ursinus* and *Otaria byronia* (Sanfelice and de Freitas, 2008). Other studies focus entirely on individual species (Brunner, 2002; de Oliveira *et al.*, 2005). The authors concluded that dimorphism was achieved through differences in both the rate and the direction of ontogenetic shape change between males and females in each species.

While these studies provide a foundation for quantitative analysis of cranial ontogeny and evolution in pinnipeds, they are relatively limited in phylogenetic breadth. Furthermore, 3D morphometric data are better suited to the complex morphology of the mammalian skull. Here, we use 3D morphometric data to quantitatively examine cranial morphology across the three extant families of pinnipeds. We test hypotheses of phylogenetic and ecological influences on cranial morphology and quantify differences in dimorphism and ontogeny within and among the three families. Specifically, we address the following questions:

1. Do differences in cranial shape correlate with phylogenetic relationships among pinnipeds?
2. Do differences in cranial shape correlate with ecological attributes of pinnipeds?

3. Do differences in cranial ontogeny reflect different reproductive strategies among pinnipeds?
4. Does cranial shape dimorphism reflect established differences in body size dimorphism across pinnipeds?

Methods

Landmarks

An Immersion Microscribe G2X digitiser with 0.2 mm accuracy was used for collecting landmark data from secured skulls. Measurements were taken from the cranium in two different views: dorsal (37 landmarks) and ventral (49 landmarks), which were later merged into a single view with a least-squares algorithm using 10 landmarks common to both views (Table 12.1, Figure 12.2). Landmarks were selected based on clear biological homology across all specimens, with emphasis on sutures, and were chosen so that all

Table 12.1 Cranial landmarks used in analyses. Landmark numbers refer to Figure 12.2. * indicates symmetrical landmarks, gathered from right and left side. + represents overlapping landmarks that were used to unify the dorsal and ventral views.

Number	Landmarks
1	Anterior interpremaxilliary suture^{+}
2	Nasal midline
3	Nasal width*
4	Premaxilla–Nasal–Maxilla suture*
5	Nasal–Frontal midline suture
6	Maxilla–Frontal–Nasal suture*
7	Jugal–Maxilla anterior dorsal suture*
8	Antorbital process*
9	Postorbital process/Interorbital width*$^{+}$
10	Jugal–Squamosal anterior suture*
11	Jugal posterodorsal process*
12	Parietal–Occipital midline suture
13	Foramen magnum dorsal extreme^{+}
14	Premaxilla–Maxilla venterolateral suture*
15	Canine anterior*
16	Canine posterior*
17	Canine labial*
18	Cheek teeth anterior*

Table 12.1 (*cont.*)

Number	Landmarks
19	Cheek teeth posterior*
20	Maxilla–Premaxilla midline suture
21	Maxilla–Palatine midline suture
22	Palatine–Maxilla lateral suture*
23	Midline between ultimate molars
24	Posterior Interpalatine suture
25	Jugal–Maxilla posteroventral suture*+
26	Jugal–Squamosal posteroventral suture*+
27	External Auditory Meatus lateral extreme*
28	Auditory Bulla anteromedial extreme *
29	Auditory Bulla posterior extreme*
30	Mastoid Process lateral extreme*
31	Mastoid Process posterior extreme*
32	Basion
33	Occipital Condyle venteromedial*+
34	Occipital Condyle dorsomedial*

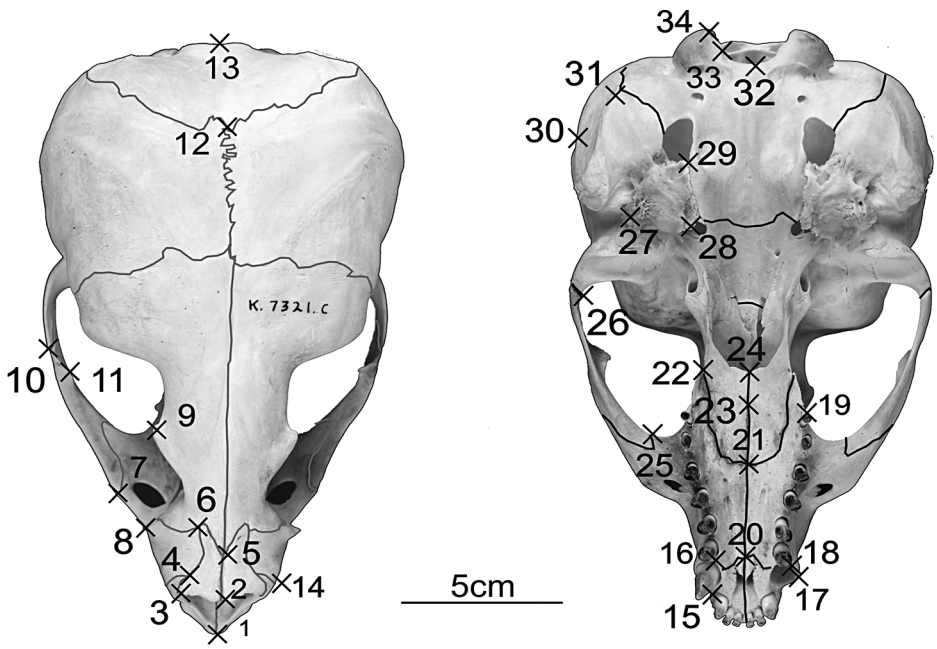

Figure 12.2 Landmarks collected and included in final analysis, shown on *Arctocephalus gazella*. Numbers correspond with landmarks listed in Table 12.1. Symmetrical landmarks are shown on one side only.

regions of the skull were taken into account. Because of the emphasis on points of clear homology, it is possible that structures of ecological or functional importance were not sampled. Analyses based on landmarks, particularly those concentrated on sutures, may well underestimate shape differences between skulls (Macleod, 1999). However, because this study considers both phylogenetic and ecological aspects of shape across a diversity of taxa, the focus on biological homology is justified.

The 10 common landmarks were widely distributed on the *x*, *y* and *z* axes in order to minimise error when merging the views (Table 12.1, Figure 12.2). Landmarks were repeated 3 times in 7 specimens for error tests, and 18 landmarks with standard deviations greater than 1 mm, on specimens ranging from 20 to 50 cm in skull length, were excluded from further analysis, leaving a total of 58 landmarks.

Specimens

Specimens were measured from the collections at the University Museum of Zoology, Cambridge and the Natural History Museum, London. Of the 34 extant pinniped species, 32 were represented, including all species of phocids and odobenids, covering 20 of 21 genera (Table 12.2). A total of 208 specimens were digitised (Appendix 12.1). Every attempt was made to sample both genders equally, with the final distribution of specimens including 36% male (74 specimens), 29% female (62 specimens), and 35% unsexed (72 specimens). Of the specimens sampled, 26% were infant and juvenile (55 specimens). The young specimens used in this study were primarily identified based on age data during collection. Additional young specimens without original data were identified based on the presence of significantly open sutures. Note that, for many species, particularly phocids, suture closure occurs well after weaning, but before sexual maturity, although more specific information is unavailable (Schulz and Bowen, 2004).

Data analysis

Cranial shape

The dorsal and ventral views were unified into one data set using 10 overlapping landmarks and a least-squares algorithm in Mathematica 6.0.1 (Wolfram Research Inc., Champaign, IL). Next, 12 midline points were used as a mirroring plane to fill in gaps in symmetrical landmarks. Both stages offered an opportunity to measure error and specimens with high error were removed from the analysis. Seventy-two specimens were removed prior to analysis due to high error or missing landmarks, leaving a total of 136 specimens analysed for 58 landmarks

Table 12.2 List of species included in analyses.

Otariidae	**Phocidae**
Arctocephalus australis	*Hydrurga leptonyx*
Arctocephalus forsteri	*Leptonychotes weddellii*
Arctocephalus galapagoensis	*Lobodon carcinophagus*
Arctocephalus gazella	*Mirounga angustirostris*
Arctocephalus phillippi	*Mirounga leonina*
Arctocephalus pusillus	*Monachus monachus*
Arctocephalus townsendi	*Monachus schauinslandi*
Arctocephalus tropacalis	*Monachus tropacalis*
Callorhinus ursinus	*Ommatophoca rossii*
Eumetopias jubata	*Cystophora cristata*
Neophoca cinerea	*Erignathus barbatus*
Otaria byronia	*Halichoerus grypus*
Phocarctos hookeri	*Histriophoca fasciata*
Zalophus californianus	*Pagophilus groenlandica*
Odobenidae	*Phoca largha*
Odobenus rosmarus	*Phoca vitulina*
	Pusa caspica
	Pusa hispida
	Pusa sibirica

(Appendix 12.1). This unified, mirrored data was then entered into Morphologika 2.5 (O'Higgins and Jones, 2006), in which Generalised Procrustes analysis and principal components analysis were conducted (Zelditch *et al.*, 2004).

Phylogenetic signal

The correlation between phylogenetic relationship and similarity in cranial shape was tested to measure the amount of phylogenetic signal in the pinniped cranium. A patristic distance matrix was constructed using a composite phylogeny. Otariid relationships follow the phylogenetic analysis of Wynen *et al.* (2001; using the position indicated for *Arctocephalus australis* group A), whereas phocid and higher-level pinniped phylogenetic relationships follow Arnason *et al.* (2006) (Otaroidea; Figure 12.1). Euclidean distances between each pair of species were calculated for each significant principal component (Table 12.3, Appendix 12.1) and used to generate four shape distance matrices. Separate distance matrices were generated for male and female specimens, and only adult specimens were included in analyses. Each shape distance matrix was then compared to the patristic distance matrix using Spearman's rank correlation analysis. Analyses were conducted in PAST (Hammer *et al.*, 2001).

Table 12.3 Eigenvalues for each significant PC axis and the five landmarks with the PC loadings that contributed to that axis. Landmark numbers correspond to positions described in Table 12.1 and shown in Figure 12.2.

PC	Eigenvalues (%)	Landmarks with highest PC loadings
1	29.4	13, 5, 33, 4, 19
2	16.8	6, 24, 9, 7, 21
3	10.7	7, 16, 15, 12, 6
4	6.04	32, 7, 19, 17, 16

Table 12.4 Significant ecological correlates of cranial shape for first four principal components using independents contrasts. + indicates significant positive correlation; − indicates significant negative correlation ($p < 0.05$). Sexual size dimorphism was calculated from male body mass divided by female body mass (kg). Marine primary productivity was measured using ^{14}C uptake and simulated fluorescence techniques (g C m^{-2} $year^{-1}$) (Ferguson and Higdon, 2006). Seasonality was calculated as the annual variation coefficient of the monthly primary productivity, averaged over 20 years, taken from measures of soil evapotranspiration in coastal weather stations (Ferguson, personal communication).

Ecological variable	PC_1	PC_2	PC_3	PC_4
Sexual size dimorphism				
Harem size				
Latitude				
Temperature (°C)				
Productivity		−		
Seasonality	+	−		−
Lactation (days)		−		
Female maturity (days)				+
Gestation (days)				
Longevity (months)				+
Interbirth (months)				
Polygamy (yes/no)				
Weaning time (months)				
Neonate (g)		−		

Ecological correlates of cranial shape

To analyse correlations of skull shape with various ecological attributes, data on 14 ecological variables were collected from the literature (Table 12.4; Reeves *et al.*,

2002; Schulz and Bowen, 2004; Ferguson and Higdon, 2006). PC scores were averaged for all specimens of each species, including males and females, and young were excluded from ecology analyses. Because closely related species have the potential to be more similar in morphology or ecology, the independent contrasts method (Felsenstein, 1985) was used. Correlation analyses were conducted in COMPARE 4.6b (Martins, 2004) with the phylogeny shown in Figure 12.1 (Wynen *et al.*, 2001; Arnason *et al.*, 2006) and a significance value of $p < 0.05$.

Ontogenetic shape change

Ontogenetic trajectories were calculated from PC1 and 2 (Figure 12.3). The length and angle were calculated trigonometrically from PC1 and PC2 scores (*X* and *Y* coordinates) of relevant specimens of known age and sex. Only species with both adult and young specimens of the same sex could be included, resulting in a representation of 18 species. Size differences between juvenile

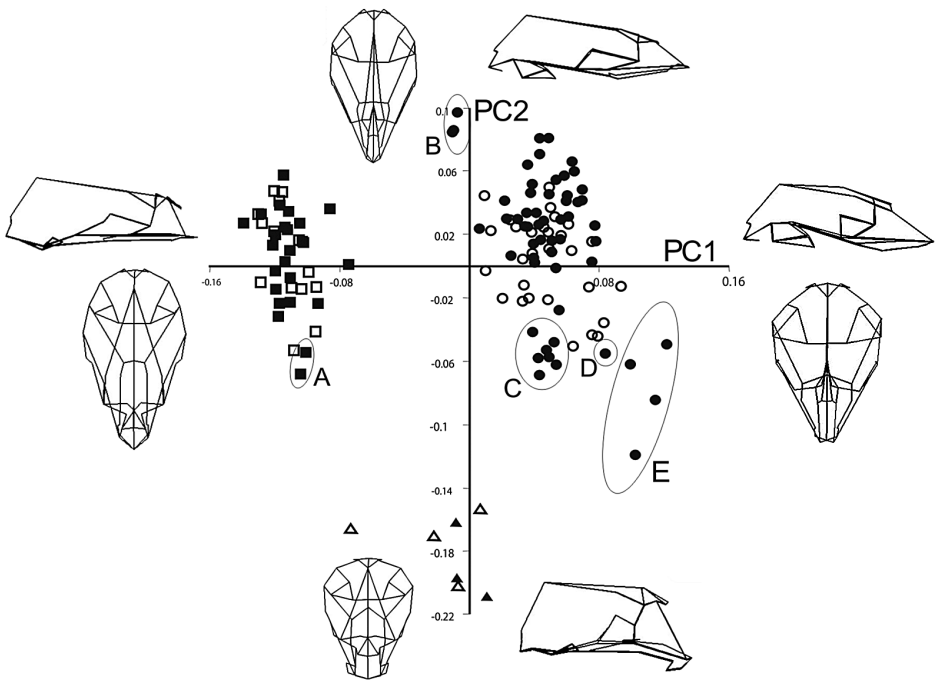

Figure 12.3 Principal components analysis displaying the first two principal components. Wireframes represent the position of landmarks in specimens at the extremes of the axes they are found next to. Symbols represent: ● phocids; ■ otariids; ▲ odobenids; open symbols: young. A, Male *Otaria byronia*; B, *Hydrurga leptonyx*; C, *Erignathus barbatus* and *Halichoerus grypus*; D, Male *Mirounga leonina*; E, *Cystophora cristata*. PC loadings and eigenvectors are provided in Table 12.3.

and adult specimens were measured using centroid size (adult/young). The length of the vector in morphospace was then compared to centroid size ratio of the two specimens with Spearman's rank correlation analysis in PAST (Hammer *et al.*, 2001). This is important to verify that longer ontogenetic trajectories were not simply produced by the uneven sampling of younger (and smaller) specimens. An unbiased data set should not show a significant correlation between ontogenetic trajectory length and centroid size.

Sexual dimorphism

Male–female trajectories on PC1 and PC2 (shape differences due to dimorphism) were calculated using a similar method as in the analysis of ontogenetic trajectories described above. Only adult specimens of known sex were included, eliminating 12 species (Appendix 12.1) from the analysis. Where multiple individuals of each sex of the same species existed all possible trajectories were plotted. An analysis was also conducted to test if the ratio of male to female centroid size correlates with degree of shape dimorphism (vector length) in pinnipeds (i.e. are species that are dimorphic in cranial size also dimorphic in shape?). In addition, shape dimorphism (vector length in PC1 and PC2) between males and females was plotted against published data on body mass dimorphism (Ferguson and Higdon, 2006) to compare cranial and postcranial dimorphism.

Results

Cranial shape

The first four principal components (Table 12.3 and Appendix 12.1) explained significant shape changes in the data set (29%, 17%, 11%, and 6% of the total variance, respectively). The first two principal components (Figure 12.3) primarily reflected phylogeny, as the three families grouped into very distinct areas of the morphospace that did not overlap. PC1 represented otariid-like morphology at the negative end to phocid-like morphology at the positive end. Species with extremely negative scores on PC1, such as *Callorhinus ursinus*, had an enlarged palate, broad interorbit and reduced auditory bullae. At the positive end of the PC1 axis, species, such as *Cystophora cristata*, showed narrow, posteriorly placed nasal and interorbit and inflated auditory bullae. The highest PC loadings for PC1 (Table 12.3) were concentrated in the rostral region and around the occipital region. PC2 (Figure 12.3) (16.8%) represented shape differences between otariids and phocids at the positive end to walruses at the negative end. *Hydrurga leptonyx* represented the positive extreme of PC2, with a pointed snout and more slender nasal and interorbit region. Walrus

specimens, which occupied the negative end of PC2, had a wide nasal opening, large canines, and broad nasals. Dominant PC2 loadings were located in the palate and snout (Table 12.3). Suction-feeding species (*Odobenus rosmarus*, *Erignathus barbatus*) had more negative scores on PC2 and another dietary specialist, *Hydrurga leptonyx*, had a more negative PC1 score than the other phocids.

Phocid specimens covered a wider range of morphospace than otariids did, reflecting the greater diversity in cranial morphology in phocids. Although the three pinniped families are clearly distinct in morphospace, there were some species that deviated markedly from their respective clade's space. The phocids *C. cristata*, *Halichoerus grypus*, *E. barbatus* and the otariid *Otaria byronia* had particularly negative PC2 scores. This indicated morphological convergence with the odobenids. One phocid, *H. leptonyx*, had a particularly negative PC1 score, indicating a more otariid-type skull morphology than observed in other phocids.

PC3 and PC4 (Figure 12.4) did not show the strong phylogenetic groupings apparent in PCs 1 and 2. On these axes, odobenids, phocids, and otariids all

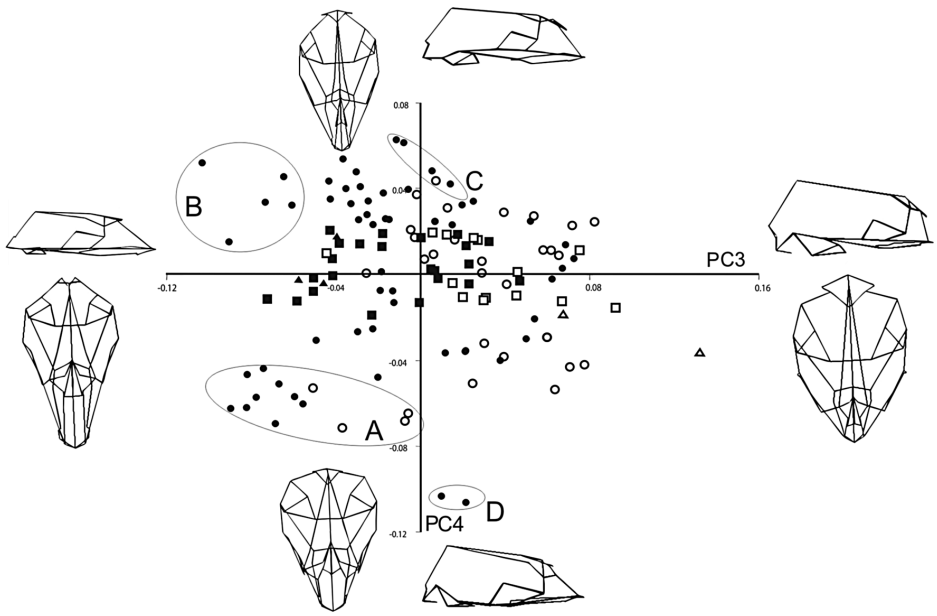

Figure 12.4 Principal components three and four. Symbols represent: ● phocids; ■ otariids; ▲ odobenids; open symbols: young. A, *Hydrurga leptonyx* and *Lobodon carcinophagus*; B, *Halichoerus grypus*; C, *Erignathus barbatus*; D, *Ommatophoca rossi*. PC loadings and eigenvectors are provided in Table 12.3.

occupied similar space. PC_3 had a strong ontogenetic component and young from all three clades fell towards the positive end of the axis. At the positive end of PC_3 was an odobenid foetus with small canines and a reduced frontal region. *H. grypus*, *H. leptonyx,* and *Lobodon carcinophagus* adults occupied the negative end of PC_3. They had a longer skull, enlarged sagittal crest and canines. High PC loadings (Table 12.3) were concentrated on the canines and snout. PC_4 (Figure 12.4) was dominated by shape change within the phocids, ensuring otariids and odobenids clustered around zero. *Ommatophoca rossi* was found at the negative end of PC_4, and *E. barbatus*, the phocid suction-feeder (Marshall *et al.*, 2008), at the positive end. Dominant PC_4 loadings (Table 12.3) involved the basion and dentition, which was reflected in the clear separation of dietary groups on these axes. In addition to *E. barbatus*, filter feeders and large prey feeders formed a cluster away from their sister taxon, *Leptonychotes weddelli*, on the negative end of PC_3 and PC_4.

Phylogenetic signal

The analyses of the relationship between phylogeny and cranial shape showed several significant correlations. For male cranial shape there were significant correlations between phylogeny and PC_1 ($p < 0.001$) and PC_4 ($p < 0.001$). Female cranial shape was significantly correlated with phylogeny on PC_1 ($p < 0.001$) and PC_2 ($p = 0.002$).

Ecological correlates of cranial shape

After removal of phylogenetic effects, seasonality was the only variable to correlate significantly with PC_1, showing a positive correlation (Table 12.4). Seasonality and productivity correlated negatively with PC_2. The reproductive variables of neonate mass and lactation time were also negatively correlated with PC_2 scores.

There were no correlations with PC_3 suggesting this axis is not greatly influenced by ecology (Table 12.4). Longevity and age to female maturity were both positively correlated with PC_4 scores. Also, seasonality correlated negatively with this axis.

Ontogenetic shape change

The ontogenetic trajectories (arrows drawn from young to adults; Figure 12.5a) varied depending on the distance of the adult members of a species from the mean shape for its respective family. Species with adult morphologies closer to the mean shape for each family (low to moderate

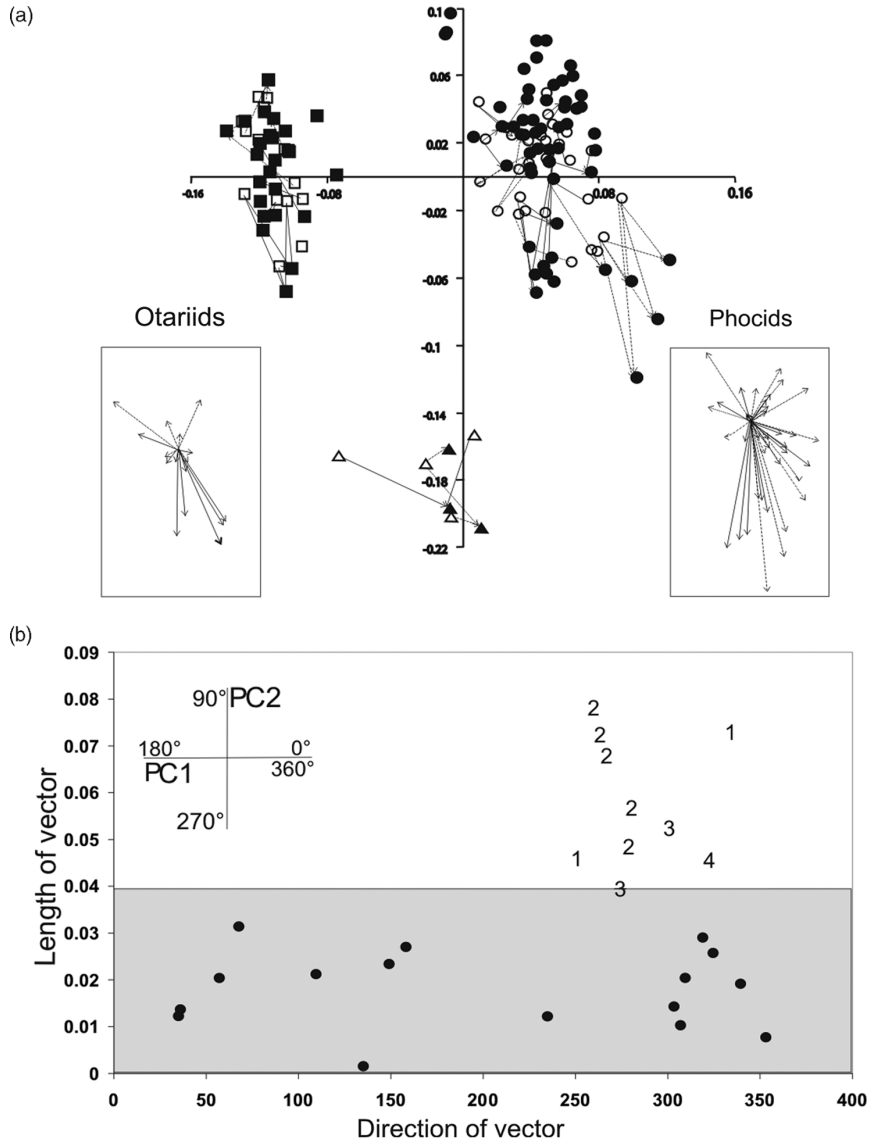

Figure 12.5 a, Ontogenetic trajectories (young to adult) plotted onto the first two principal components axes. Solid arrows are between specimens of the same sex, dotted arrows are between one or two specimens of unknown sex. Only specimens of known sex are included in b. Boxes show all ontogenetic trajectories for the respective family, re-oriented to the same origin. Symbols represent: ● phocids; ■ otariids; ▲ odobenids; open symbols: young. b, Plot of direction of ontogenetic trajectory against degree of ontogenetic shape change. Direction is measured as angle anticlockwise from the positive PC_2 axis. A key relating angle to direction on the PC_1 and PC_2 axes is shown in the top left. Degree of shape change is measured as length of the vector. The grey area marks specimens that show short ontogenetic trajectories in all directions. The white area indicates specimens with long (greater than 0.4) ontogenetic trajectories and are concentrated between 250 and 350 degrees. 1: *Odobenus rosmarus*, 2: *Halichoerus grypus*, 3: *Otaria byronia*, 4: *Lobodon carcinophagus. Erignathus barbatus* and *Cystophora cristata* were not included in part B due to lack of sex data.

ontogenetic shape changes) tended to have shorter trajectories. These species also had a wider distribution of directions of the ontogenetic trajectories. However, longer trajectories were consistently oriented in the direction of negative PC_2 values (Figure 12.5b). Specifically, for adults with highly negative PC_2 scores (convergent on odobenid morphology), the young of those species usually displayed more generalised cranial morphology, near the mean shape for their family, resulting in long trajectories in the direction of negative PC_2 (Figure 12.5a).

Plotting length of trajectory against relative size difference between young and adult specimens (ratio of adult to young centroid size) produced no significant correlation (Spearman's $r=0.0054$, $p=$n.s.). This result demonstrated that the ontogenetic patterns observed in Figure 12.5 were not a product of sampling bias.

Sexual dimorphism

Dimorphism vectors (Figure 12.6a) showed patterns similar to those found in ontogenetic trajectories (Figure 12.5a) described above. Low to moderate differences in cranial shape dimorphism were heterogenous in orientation (Figure 12.6b). However, phocids and otariids with negative scores on PC_2 because of morphological adaptations relating to mating display showed longer distances between males and females (Figure 12.6a). These species (*C. cristata*, *O. byronia*, *Mirounga leonina*) all showed vectors aligned towards negative PC_2 direction, toward odobenid morphospace, in a similar manner to the ontogenetic trajectories described above (Figure 12.6a).

Dimorphism distance was significantly correlated with male/female centroid size ratio ($r=0.45$, $p=0.002$), indicating that species showing large dimorphic differences in cranial size also display large dimorphic differences in cranial shape.

In contrast, results suggested dissociation between cranial shape dimorphism and body mass dimorphism in some species (Figure 12.7). Most phocids and the odobenids displayed low to moderate cranial shape dimorphism (0–0.4) and low body size dimorphism (1–2). On the other hand, most otariids showed higher body size dimorphism (3–4) over a similar range of cranial shape dimorphism (0–0.4). *M. leonina* showed extremely large values on both axes. *C. cristata* and *O. byronia* grouped together as having lower body size dimorphism (1–2) but very high shape dimorphism (0.5–0.8).

Discussion

Pinniped families showed strong phylogenetic signal in their cranial morphology (Figure 12.3). Significant correlations between phylogeny and

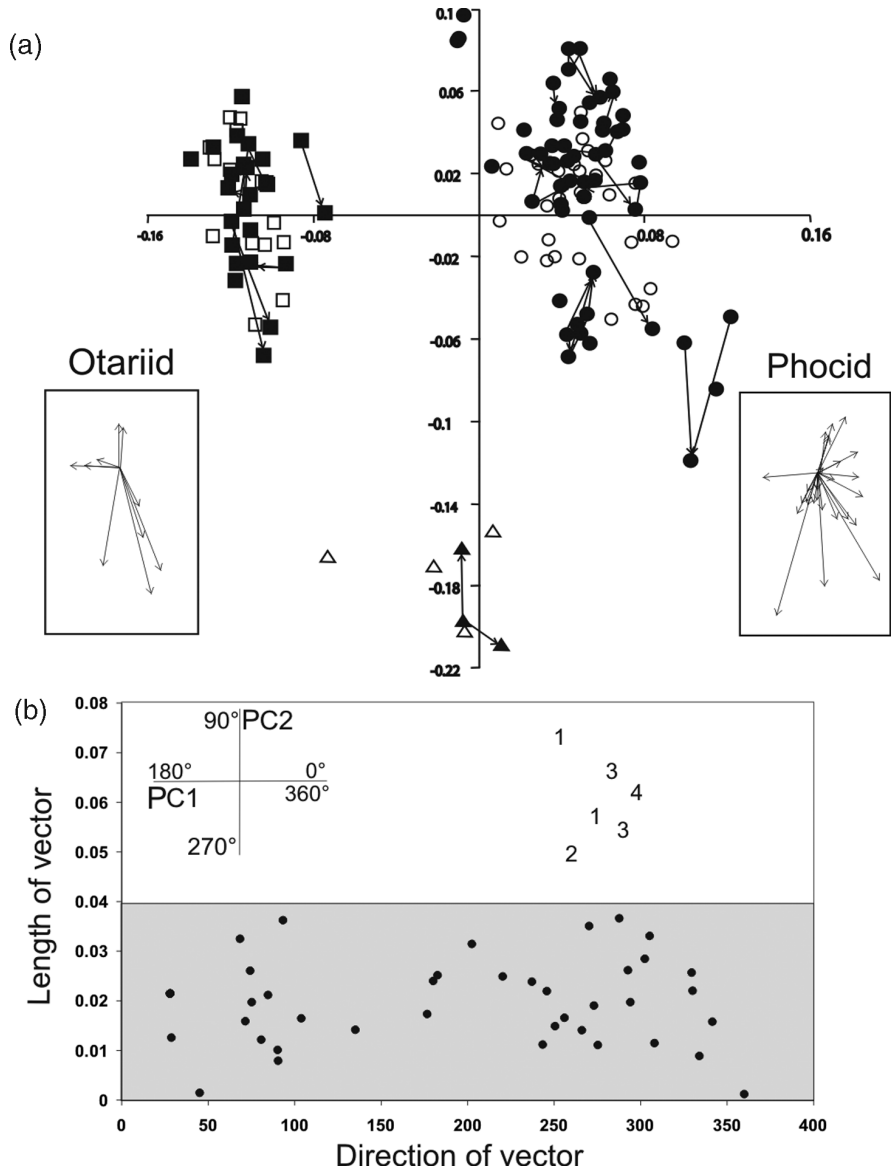

Figure 12.6 a, Distances plotted from females to males onto the first two principal components. Boxes show all vectors for the respective family, re-oriented to the same origin. Symbols represent: ● phocids; ■ otariids; ▲ odobenids; open symbols: young. b, Plot of direction of dimorphic shape difference against degree of dimorphic shape difference. Direction is measured as the angle anticlockwise from the positive PC_2 axis. A key relating angle to direction on PC axis is shown in the top left. Degree of difference is measured as the length of the vector. The grey area marks specimens that show short vectors in all directions. The white area indicates specimens with long (greater than 0.4) vectors and are concentrated between 250 and 300 degrees. 1: *Cystophora cristata*, 2: *Arctocephlalus gazella*, 3: *Otaria byronia*, 4: *Mirounga leonina*.

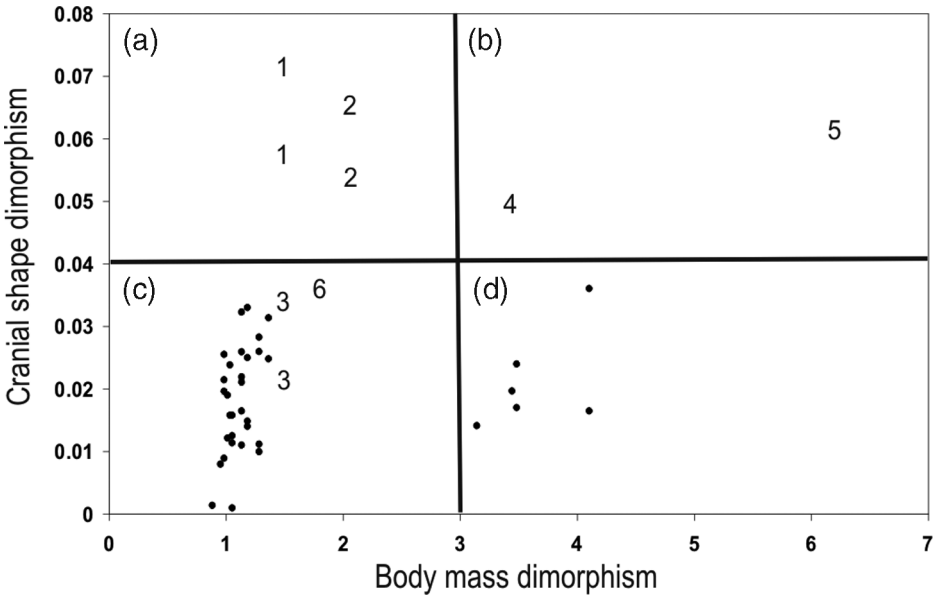

Figure 12.7 Plot showing body mass dimorphism against cranial shape dimorphism. Body mass dimorphism is the ratio of female to male body mass for each species, collected from the literature (Ferguson and Higdon, 2006). Cranial shape dimorphism is measured as the length of the vector between male and female specimens on PC_1 and PC_2 (Figure 12.6a). Specimens plot into four quadrants: a, high cranial shape dimorphism and low body mass dimorphism; b, high cranial and body mass dimorphism; c, low cranial and body mass dimorphism; and d, low cranial shape dimorphism and high body mass dimorphism. 1: *Cystophora cristata*, 2: *Otaria byronia*, 3: *Odobenus rosmarus*, 4: *Arctocephalus gazella*, 5: *Mirounga leonina*, 6: *Arctocephalus australis*. All phocids except those specified are found in sector C. Sector D contains solely otariids.

cranial shape on multiple principal components indicated that phylogeny was the most dominant influence on cranial morphology. However, cranial morphology did not reflect the considerable ecological overlap between phocids and otariids. This pattern possibly reflects morphological differences that evolved early in the histories of these clades, although fossil taxa need to be included to determine when these distinct areas of morphospace were invaded. The results presented here suggest a number of potential hypotheses that could be tested with fossil data. First, the marked phylogenetic separation among the three clades may be partially due to the loss of intermediate forms, particularly given the relatively large otariid and odobenid stem groups. Second, the smaller range of otariid morphological diversity may also reflect the greater loss of otariid

taxonomic diversity through extinction, as the crown group represents a relatively small proportion of the total group for otariids. By contrast, extant phocids represent many basal branches and so the crown group includes many more extinct species than that of the otariids (Deméré *et al.*, 2003). Third, the basal split of monachine and phocine phocids (20 Mya) was not reflected in skull morphology on PC1 or 2 (Figure 12.3). For example, *C. cristata* (a phocine) and *M. leonina* (a monachine) plotted very near to each other on PC1 and PC2 (Figure 12.3). This result suggests either that there has been much morphological convergence between these groups since they diverged, or that there was relatively little morphological differentiation associated with their divergence.

Although the families of pinnipeds displayed remarkably different cranial morphology, some species were conspicuously positioned away from position of the standard phylogenetic grouping in morphospace. These species displayed morphological convergence that bridged the morphospace defined by the three pinniped families (Figure 12.3). Convergence was more common in the phocids than in the otariids, reflecting their greater ecological diversity and more extreme specialisations. These examples of convergence can be classified into those due to diet and those due to mating displays.

The most apparent example of morphological convergence reflecting similarity in diet is observed in *E. barbatus*. This species had a particularly low score on the PC2 axis (Figure 12.3) of around −0.06, approaching the region of morphospace occupied by odobenids (the mean for odobenids is −0.18), than other phocids (the mean for phocids is ∼0). This species shares a similar diet with walruses in feeding within the sediment on fish and invertebrates, and a recent study showed that *E. barbatus* uses suction feeding 96.3% of time whilst feeding underwater (Marshall *et al.*, 2008). This result shows there are aspects of cranial morphology adapted for suction feeding that have evolved independently in both phocids and odobenids.

H. grypus also grouped very closely with *E. barbatus* in morphospace (Figure 12.3). However, this species is not solely a sediment feeder, but eats a wider range of fish including bottom-dwellers, crustaceans, and molluscs (King, 1983). The method it uses for feeding on molluscs (crunching or suction-feeding) is unclear, but these results suggest that it has some adaptations for sediment feeding, despite retaining a generalist diet.

In constrast to those species that converge ecologically and morphologically with walruses, *H. leptonyx* represents a phocid that may converge toward otariids. *H. leptonyx* was located in between the phocid and otariid cluster on PC1, with a mean PC score of −0.01, compared to a range of 0.01–0.08 for other phocids and a range of −0.07 to −0.14 for otariids (Figure 12.3).

This position reflects more otariid-like morphology than observed in other phocids. This unusual morphology may relate to the fact that *H. leptonyx* is the only pinniped to specialise on large, warm-blooded prey (Reeves *et al.*, 2002). However, many otariids incorporate large prey as a small part of their diet. The otariid skull is generally more robust than the typical phocid skull, which may reflect the necessity to cope with the large forces associated with large-prey feeding, and may have evolved convergently in *H. leptonyx* for the same purpose.

In addition to convergence relating to diet, several pinnipeds displayed unusual morphologies related to mating displays. The most conspicuous example of cranial adaptations for sexual displays are found in *C. cristata*. This species had the lowest score among phocids on PC2 (−0.012, Figure 12.3). The large dimorphism distance on PC2 between females and males (female average −0.6) (Figure 12.6a) supported the interpretation that this convergence toward odobenid morphospace was related to mating strategy. Male *C. cristata* have a large proboscis that is used in mating displays, including an internal nasal membrane that can be inflated to produce a large, red, facial bladder (Reeves *et al.* 2002). This is facilitated by a wider nasal opening, which is superficially similar to the wide rostrum observed in walruses. However, females also had a much lower score on this axis (Figure 12.3) than the young (−0.03) for reasons that are not apparent.

M. leonina males also fall out relatively low on the PC2 axis (−0.06; Figure 12.3). Male *M. leonina* are the only other phocid species to have evolved a proboscis, convergently with *C. cristata*, although they do not have a facial bladder.

While most unusual morphologies were observed in phocids, *O. byronia* males were significantly more negative on PC2 than the other otariids (−0.07; Figure 12.3), consistent with qualitative reports (King, 1983) describing male *O. byronia* as having a distinctive upturned snout. *O. byronia* feed on seafloor fish and cephalopods (Reeves *et al.*, 2002), and some authors (Adam and Berta, 2002) have suggested *O. byronia* skulls show characteristics associated with suction feeding (lengthening of the hard palate and robust pterygoid hamuli), although experimental confirmation of their feeding mechanism is not available. However, results presented here showing that female and young *O. byronia* cluster near other otariids, around 0.0 on PC2 (Figures 12.3 and 12.6a), support the interpretation of cranial convergence of *O. byronia* with *O. rosmarus* as due to sexual dimorphism and not related to diet.

These results (Figure 12.3) suggest that walrus morphospace was a popular direction for cranial morphological evolution in the pinnipeds. This morphology may have represented a common adaptation for accessing the sediment–water interface (e.g. *E. barbatus*, *H. grypus*), in order to expand their range of

feeding opportunities. Alternatively, it may relate to food processing and stages in the independent evolution of suction feeding. Modifications to the cranium for mating displays were also concentrated in the rostral region, often resulting in dimorphic convergence of males in the direction of walrus morphospace.

This repeated pattern of phocids and otariids converging in the direction of walrus morphospace for modifications related to both diet and sexual display suggests that the pinniped morphology may be constrained from exploring other regions of cranial morphospace. Possibly, this repeated modification of primarily the rostral region across all extant pinniped groups, and for both feeding and mating displays, may reflect constraints to maintain a hydrodynamic form. More specifically, transformations of the rostral region may have occurred independently multiple times because vertebrates with postcrania that are highly adapted for swimming cannot drastically modify their skeleton for use in mating displays or prey capture. This constraint would explain why mating displays in pinnipeds are limited to the nasal region. Furthermore, cranial dimorphism may be especially significant for species in which size dimorphism is limited by adaptations for large female body size due to low temperatures, such as *O. byronia* (Ferguson and Higdon, 2006), discussed further below.

Ecological correlates of cranial shape

Seasonality correlated significantly with three of the four significant principal component axes (PC1, 2 and 4; Table 12.4). This may reflect differences between ice-breeding species, living in highly seasonal environments, and those living in more temperate conditions. On PC1 this correlation most likely reflected the presence of phocids at high latitudes. Phocids are primarily found at higher latitudes and in polar regions, while otariids inhabit primarily equatorial to mid-latitude regions (Ferguson and Higdon, 2006). This geographical pattern reflects the fact that otariids are excluded from the most high-latitude environments by their inability to breed on ice, while many phocids are ice-breeders (Schulz and Bowen, 2004).

Productivity as well as seasonality correlated with PC2, suggesting that cranial shape was highly influenced by availability of resources at the base of the food chain. In addition, reproductive factors were correlated with cranial morphology on PC2 (Table 12.4). Large male, female, and neonate body masses were demonstrated in those species converging on odobenid space. Longer lactation times accompanied convergence in some species and this result is likely to be driven by extremely long lactation in walruses. Lactation time is

related to female mass as larger fat stores facilitate a longer period of milk production (Schulz and Bowen, 2004).

PC_3 scores did not correlate with any ecological variables, perhaps reflecting the strong influence of ontogeny on this axis. Correlation of PC_4 scores with age to maturity and longevity suggest life history is an important influence on cranial morphology.

It is interesting to note that ecological specialisations are found exclusively in those pinnipeds native to the high latitudes (above 70° north or south; Ferguson and Higdon, 2006) and high seasonality environments. This may present an environment in which a specialist feeding habit is favourable to the generalist approach seen in all other locations. Resources at higher latitudes are scarce, so specialised ecologies and related morphologies may allow these pinnipeds to exploit the food sources available to them more effectively than their generalist relatives can.

Ontogenetic shape change

The analysis of ontogenetic shape change (Figure 12.5) revealed that there was no consistent shape trajectory for cranial growth across pinnipeds or within phocids and otariids. It did, however, highlight an interesting relationship between morphological convergence on odobenid space and length and direction of ontogenetic trajectory in phocids and otariids. First, it showed that all these species were undergoing similar skull shape changes during growth (Figure 12.5a). Second, the results showed that species that converge towards walrus cranial shape had a greater difference in young and adult morphology than non-convergent species (Figure 12.5b). In these species, young specimens showed morphology more similar to that of the rest of their family (Figure 12.5a). This pattern means that the unusual morphology observed in adults was only achieved after weaning and required extreme modifications in cranial shape during growth. This shift suggests that the morphological traits observed are only required during the later stages of their lives, possibly representing sexual selection or differences in juvenile and adult diets.

In the cases of *C. cristata*, *M. leonina,* and *O. byronia*, the morphological shift may reflect the development of sexual characteristics. In *E. barbatus* and *H. grypus*, however, which converge on odobenid space due to diet, it is possible that these ontogenetic shifts reflect changes in diet after weaning. For sediment feeders, the ability to dive deeply and for prolonged periods may require further development and hence a change in diet. Unfortunately, there are currently little data available regarding the post-weaning diets of pinniped young that would be required to test this hypothesis.

Sexual dimorphism

The analyses of cranial dimorphism (Figure 12.6) demonstrated that there is a strong positive correlation between size and shape dimorphism of pinniped crania. While the data presented here lack the ontogenetic resolution needed for testing specific hypotheses of allometry, the correlation between cranial shape and cranial size dimorphism may simply reflect allometric differences between adult males and females. In at least a few cases, such as *M. leonina*, overlapping ontogenetic (Figure 12.5a) and dimorphism (Figure 12.6a) trajectories provide tentative support for this hypothesis. However, in many cases, such as *C. cristata*, the trajectories are not coordinated, suggesting that shape dimorphism is not simply a consequence of allometric differences between adult males and females.

A recent study of ontogeny and dimorphism in three species of otariids, *O. byronia*, *C. ursinus,* and *A. australis* specifically tested the role of allometry in generating cranial shape dimorphism. Their results demonstrate that shape dimorphism may simply reflect allometry in *C. ursinus*, but that allometry alone cannot explain the shape differences observed in *O. byronia* and *A. australis* (Sanfelice and de Freitas, 2008). Their detailed ontogenetic study showed that dimorphism in *O. byronia* is achieved very early in development, resulting in shape differences even between male and female juveniles. Strikingly, the authors report that the rate of male cranial growth is three times greater than that of females, implicating a strong heterochronic shift in the evolution of cranial dimorphism in *O. byronia*. Improved data from ontogenetic series of a diverse sample of pinnipeds, particularly those species highlighted in this study for converging on odobenid morphology through ontogenetic shape changes, will be essential to rigorously test the role of allometry and heterochrony in cranial shape dimorphism.

It is also notable that *C. cristata*, *M. leonina* and *O. byronia* all showed remarkably similar trajectories of shape dimorphism (Figure 12.6a), despite representing a wide phylogenetic range (otariid and monachine and phocine phocid). These species also displayed the most marked differences in male–female morphology (Figure 12.6b). As noted above, in some of the species that converge on walrus cranial morphology, such as *O. byronia*, dimorphic shape differences (Figure 12.6a) were similar in direction to the ontogenetic trajectories (Figure 12.5a), with adult females that are similar in cranial morphology to juvenile specimens. This result is consistent with previous analyses demonstrating that adult female *O. byronia* share a very similar morphology with subadults of both sexes, whereas adult male morphological traits arise well before adulthood (Sanfelice and de Freitas, 2008). In the results presented here, these

differences between males and females primarily reflect the development of sexual characteristics, such as a proboscis or facial bladder, in adult males, driving their convergence on odobenid cranial morphology.

Interestingly, our study demonstrated that large dimorphic shape differences in *C. cristata* and *O. byronia* were not accompanied by increased body mass dimorphism (Figure 12.7). In fact, these species showed amongst the lowest body size dimorphism, suggesting that body mass dimorphism and cranial shape dimorphism may represent alternative strategies. For example, *O. byronia* inhabits environments with very low temperatures (−14°C average, Ferguson and Higdon, 2006) and also has relatively large female body size. One possibility is that the observed low body mass dimorphism (2.08) (Figure 12.7) may relate to a lower limit to female body size due to colder environments. Alternatively, the trade-off between cranial shape dimorphism and body size dimorphism may relate to the relative importance of display to fighting in male competition. Cranial shape dimorphism is expected to be more pronounced in species using elaborate male displays, such as facial bladders, while body mass dimorphism may be more common in species in which male fighting dominates.

Lastly, the analyses of dimorphism presented here demonstrated that intraspecific shape differences among males and females were large compared even to interspecific differences (Figure 12.6a). While most terrestrial carnivorans express dimorphism through size differences, the large cranial shape dimorphism observed in pinnipeds here emphasises the importance of cranial morphology to multiple purposes in pinniped evolution. Pinnipeds may place unusual emphasis on the cranium for mating displays and prey-capture adaptations, such as suction or filter feeding, because the extreme specialisation of the postcranium for swimming reduces its utility in other tasks. Further analyses including fossil taxa would be essential to understanding the shift of multiple functions, such as prey-capture and mating displays, to the cranium during the terrestrial to marine transition in pinniped evolution.

Conclusions

The most striking pattern observed in this quantitative analysis of cranial morphology across extant pinnipeds is the repeated evolution of feeding and mating specialisations that converge towards odobenid morphology. The common evolutionary and developmental trajectories observed here suggest that specialisations for an aquatic lifestyle may constrain the range of functionally viable morphospace available to pinnipeds, reflected in their concentration on adaptations in the rostral region. While the three extant pinniped families

occupy distinct areas of morphospace, multiple phocids and otariids independently converge toward odobenid cranial morphology in adaptations related to both diet and mating display. Ontogenetic analyses suggest that these shifts occur primarily during the juvenile growth phase, requiring large alterations in morphology during development, likely due to dietary changes or sexual maturation. Lastly, some species illustrate a trade-off between body size dimorphism and cranial shape dimorphism, perhaps related to differences in mating behaviour or habitat among pinnipeds.

Secondary adaptations to the aquatic realm include some of the most compelling examples in vertebrate evolution (Uhen, 2007). However, pinniped evolutionary morphology remains understudied in comparison to other aquatic mammals. This study demonstrates that the unique reproductive and ecological strategies pursued by pinnipeds are matched by several interesting patterns in the morphological evolution of the pinniped cranium, providing a promising avenue for future studies of major evolutionary transitions.

Acknowledgements

We are indebted to Matt Lowe (University Museum of Zoology Cambridge) and Richard Sabin (Natural History Museum, London) for access to specimens and extensive help during data collection. S. H. Ferguson kindly provided details of ecological measures. A. Piotrowski provided helpful discussion of climatic measures. V. Weisbecker generously read and commented on an early version of this manuscript.

REFERENCES

Adam, P. J. and Berta, A. (2002). Evolution of prey capture strategies and diet in the Pinnipedimorpha (Mammalia, Carnivora). *Oryctos*, **4**, 83–107.

Arnason, U., Gullberg, A., Janke, A., *et al.* (2006). Pinniped phylogeny and a new hypothesis for their origin and dispersal. *Molecular Phylogenetics and Evolution*, **41**, 345–54.

Berta, A. and Adam, P. J. (2001). Evolutionary biology of pinnipeds. In *Secondary Adaptation of Tetrapods to Life in Water*, ed. J. -M. Mazin and V. de Buffrénil. Munich: Verlag Dr. Friedrich Pfeil, pp. 235–60.

Berta, A., Ray, C. E. and Wyss, A. R. (1989). Skeleton of the oldest known pinniped, *Enaliarctos mealsi*. *Science*, **244**, 60–62.

Bininda-Edmonds, O. R. P. and Gittleman, J. L. (2000). Are pinnipeds functionally different from fissiped carnivores? The importance of phylogenetic comparative analyses. *Evolution*, **54**, 1011–23.

Bininda-Emonds, O. R. P., Gittleman, J. L. and Kelly, C. K. (2001). Flippers versus feet: comparative trends in aquatic and non-aquatic carnivores. *Journal of Animal Ecology*, **70**, 386–400.

Brunner, S. (1998). Cranial morphometrics of the southern fur seals *Arctocephalus forsteri* and *A. pusillus* (Carnivora: Otariidae). *Australian Journal of Zoology*, **46**, 67–108.

Brunner, S. (2002). Geographic variation in skull morphology of adult steller sea lions (*Eumetopias jubatus*). *Marine Mammal Science*, **18**, 206–22.

Brunner, S. (2003). Fur seals and sea lions (Otariidae): identification of species and taxonomic review. *Systematics and Biodiversity*, **1**, 339–439.

Brunner, S., Shaughnessy, P. D. and Bryden, M. M. (2002). Geographic variation in skull characters of fur seals and sea lions (family Otariidae). *Australian Journal of Zoology*, **50**, 415–38.

de Oliveira, L. R., Hingst-Zaher, E. and Stenghel Morgante, J. (2005). Size and shape sexual dimorphism in the skull of the South American fur seal, *Arctocephalus australis* (Zimmerman, 1783) (Carnivora: Otariidae). *Latin American Journal of Aquatic Mammals*, **4**, 27–40.

Deméré, T. A., Berta, A. and Adam, P. J. (2003). Pinnipedimorph evolutionary biogeography. *Bulletin of the American Museum of Natural History*, **279**, 32–76.

Felsenstein, J. (1985). Phylogenies and the comparative method. *American Naturalist*, **125**, 1–15.

Ferguson, S. H. and Higdon, J. W. (2006). How seals divide up the world: environment, life history, and conservation. *Oecologia*, **150**, 318–29.

Flynn, J. J., Finarelli, J. A., Zehr, S., Hsu, J. and Nedbal, M. A. (2005). Molecular phylogeny of the Carnivora (Mammalia): assessing the impact of increased sampling on resolving enigmatic relationships. *Systematic Biology*, **54**, 317–37.

Hammer, O., Harper, D. A. T. and Ryan, P. D. (2001). PAST: palaeontological statistics software package for education and data analysis. *Palaeontologia Electronica*, **4**, 9 pp.

King, J. E. (1983). *Seals of the World*. London: British Museum (Natural History), 154 pp.

Kovacs, K. M. and Lavigne, D. M. (1992). Maternal investment in otariid seals and walruses. *Canadian Journal of Zoology – Revue Canadienne de Zoologie*, **70**, 1953–64.

Macleod, N. (1999). Generalizing and extending the eigenshape method of shape space visualization and analysis. *Paleobiology*, **25**, 107–38.

Marshall, C., Kovacs, K. M. and Lydersen, C. (2008). Feeding kinematics, suction and hydraulic jetting capabilities in bearded seals (*Erignathus barbatus*). *Journal of Experimental Biology*, **211**, 699–708.

Martins, E. P. (2004). COMPARE, version 4.6b: computer programmes for the statistical analysis of comparative data. Department of Biology, Indiana University, Bloomington, IN.

Muizon, C. D. E. (1982). Phocid phylogeny and dispersal. *Annals of the South African Museum*, **89**, 175–213.

O'Higgins, P. and Jones, N. (2006). Morphologika: tools for statistical shape analysis. Hull: York Medical School. http://hyms.fme.googlepages.com/resources.

Reeves, R., Stewart, B. S., Clapham, P. J. and Powell, J. A. (2002). *Sea Mammals of the World*. London: A & C Black Publishers, 528 pp.

Repenning, C. A. (1976). Adaptive evolution of sea lions and walruses. *Systematic Zoology*, **25**, 375–90.

Rybczynski, N., Dawson, M. R. and Tedford, R. H. (2009). A semi-aquatic mammalian carnivore from the Miocene epoch and origin of Pinnipedia. *Nature*, **458**, 1021–24.

Sanfelice, D. and de Freitas, T. R. O. (2008). A comparative description of dimorphism in skull ontogeny of *Arctocephalus australis*, *Callorhinus ursinus* and *Otaria byronia* (Carnivora: Otariidae). *Journal of Mammalogy*, **89**, 336–46.

Sato, J., Wolsan, M., Suzuki, H., *et al.* (2006). Evidence from nuclear DNA sequences sheds light on the phylogenetic relationships of Pinnipedia: single origin with affinity to Musteloidea. *Zoological Science*, **23**, 125–46.

Schulz, T. M. and Bowen, W. D. (2004). Pinniped lactation strategies: evaluation of data on maternal and offspring life history traits. *Marine Mammal Science*, **20**, 86–114.

Schulz, T. M. and Bowen, W. D. (2005). The evolution of lactation strategies in pinnipeds: a phylogenetic analysis. *Ecological Monographs*, **75**, 159–77.

Sinclair, E. H. and Zeppelin, T. K. (2002). Seasonal and spatial differences in diet in the western stock of Stellar sea lions (*Eumetopias jubatus*). *Journal of Mammalogy*, **83**, 973–90.

Uhen, M. D. (2007). Evolution of marine mammals: back to the sea after 300 million years. *Anatomical Record*, **290**, 514–22.

Williams, T. M., Rutishauser, M., Long, B., *et al.* (2007). Seasonal variability in otariid energetics: implications for the effects of predators on localized prey resources. *Physiological and Biochemical Zoology*, **80**, 433–43.

Wynen, L. P., Goldsworthy, S. D., Insley, S. J., *et al.* (2001). Phylogenetic relationships within the eared seals (Otariidae: Carnivora): implications for the historical biogeography of the family. *Molecular Phylogenetics and Evolution*, **21**, 270–84.

Wyss, A. R. (1988). Evidence from flipper structure for a single origin of pinnipeds. *Nature*, **334**, 427–28.

Zelditch, M., Swiderski, D., Sheets, H. D. and Fink, W. (2004). *Geometric Morphometrics for Biologists: A Primer*. Boston, MA: Elsevier Academic Press, 416 pp.

Appendix 12.1 Table of specimens included in analyses and PC scores for each specimen on the first four principal component axes.

Genus	Species	Sex	Age	Specimen	PC1	PC2	PC3	PC4
Arctocephalus	*australis*	F	Adult	01984919	−0.0859	0.0363	−0.0250	−0.0249
Arctocephalus	*australis*	M	Adult	019501114l	0.0746	0.0009	−0.0192	0.0106
Arctocephalus	*forsteri*	?	Young	K7422	−0.1212	0.0474	0.0439	−0.0029
Arctocephalus	*gazella*	F	Adult	K7321D	−0.1122	0.0343	0.0059	−0.0083
Arctocephalus	*gazella*	F	Subadult	K7321C	−0.1176	0.0425	0.0300	−0.0123
Arctocephalus	*gazella*	F	Subadult	K7321A	−0.1049	0.0165	0.0138	−0.0075
Arctocephalus	*gazella*	M	Adult	K73421L	−0.1032	0.0159	−0.0021	−0.0172
Arctocephalus	*gazella*	M	Adult	K7321M	−0.1201	−0.0152	−0.0014	−0.0171
Arctocephalus	*philippi*	?	Adult	01883118l	−0.1283	0.0330	−0.0299	0.0114
Arctocephalus	*pusillus*	?	?	K7429	−0.1141	0.0244	0.0206	0.0002
Arctocephalus	*pusillus*	F	Adult	K7361	−0.1140	0.0024	0.0039	0.0013
Arctocephalus	*pusillus*	F	Adult	01927728	−0.1126	0.0226	−0.0005	0.0152
Arctocephalus	*pusillus*	M	Adult	K7426	−0.1168	0.0382	−0.0189	0.0169
Arctocephalus	*tropacalis*	F	Adult	019553148	−0.1106	0.0098	0.0303	0.0108
Arctocephalus	*tropacalis*	M	Adult	0195742311	−0.1204	0.0194	0.0048	−0.0035
Artcocephalus	*galapogoensis*	F	Adult	019912	−0.1053	0.0273	0.0197	0.0099
Callorhinus	*ursinus*	?	Young	K72272	−0.0995	−0.0041	0.0918	−0.0161
Callorhinus	*ursinus*	F	Adult	01960522	−0.1397	0.0269	0.0159	0.0150
Callorhinus	*ursinus*	M	Subadult	K7221	−0.1301	0.0328	0.0045	0.0169
Cystophora	*cristata*	?	Young	K7750	0.0823	−0.0362	0.0775	−0.0446
Cystophora	*cristata*	?	?	K7741	0.1141	−0.0850	−0.0302	−0.0337
Cystophora	*cristata*	?	Young	K7742	0.0930	−0.0131	0.0391	−0.0445

Cystophora	*cristata*	F	Adult	K7745	0.1210	−0.0496	−0.0126	−0.0182
Cystophora	*cristata*	F	Adult	18446231	0.0987	−0.0627	−0.0231	−0.0321
Cystophora	*cristata*	M	Adult	332h	0.1024	−0.1201	−0.0499	−0.0387
Erignathus	*barbaratus*	?	Young	K8022	0.0638	−0.0513	−0.0107	0.0612
Erignathus	*barbaratus*	?	?	K8023	0.0530	−0.0626	−0.0112	0.0640
Erignathus	*barbaratus*	?	?	K8021	0.0495	−0.0579	−0.0072	0.0639
Erignathus	*barbaratus*	?	Young	18786191	0.0327	−0.0226	0.0079	0.0480
Erignathus	*barbaratus*	F	Adult	193710239	0.0395	−0.0417	0.0056	0.0506
Eumetopias	*jubatus*	?	?	K7081	−0.1211	0.0133	−0.0513	−0.0053
Eumetopias	*jubatus*	?	?	0195032912	−0.1180	−0.0321	−0.0517	−0.0113
Eumetopias	*jubatus*	F	Young	0195032910	−0.1203	0.0217	−0.0453	0.0082
Eumetopias	*jubatus*	F	Adult	0192510832	−0.0927	−0.0244	−0.0413	−0.0014
Eumetopias	*jubatus*	M	Adult	019507214	−0.1173	−0.0240	−0.0451	0.0070
Eumetopias	*jubatus*	M	Adult	01968891	−0.1108	−0.0229	0.0470	−0.0002
Eumetopias	*jubatus*	M	Young	0190310118	−0.1097	−0.0143	0.0308	−0.0081
Halichoerus	*grypus*	F	Adult	K7943	0.0477	−0.0532	−0.0659	0.0415
Halichoerus	*grypus*	F	Young	196151820	0.0562	0.0185	−0.0262	−0.0016
Halichoerus	*grypus*	F	Adult	196151836	0.0528	−0.0491	−0.0612	0.0304
Halichoerus	*grypus*	F	Adult	196151832	0.0429	−0.0584	−0.0737	0.0312
Halichoerus	*grypus*	M	Young	19615182	0.0337	−0.0130	0.0021	0.0086
Halichoerus	*grypus*	M	Adult	196151811	0.0551	−0.0280	−0.0908	0.0122
Halichoerus	*grypus*	M	Young	19391141	0.0367	−0.0210	0.0298	0.0080
Halichoerus	*grypus*	M	Adult	1962361	0.0438	−0.0697	−0.1032	0.0505

Appendix 12.1 (*cont.*)

Genus	Species	Sex	Age	Specimen	PC1	PC2	PC3	PC4
Histriophoca	*fasciata*	M	Subadult	19661272	0.0487	0.0111	0.0616	0.0107
Histrophoca	*fasciata*	F	Adult	19657197	0.0565	0.0294	0.0681	0.0157
Histrophoca	*fasciata*	F	Adult	19657199	0.0764	0.0159	0.0509	0.0232
Histrophoca	*fasciata*	F	Subadult	1657195	0.0627	0.0095	0.0819	0.0257
Histrophoca	*fasciata*	M	Adult	19637196	0.0753	0.0026	0.0724	0.0072
Histrophoca	*fasciata*	M	Adult	19637197	0.0507	0.0151	0.0665	0.0023
Histrophoca	*fasciata*	M	Subadult	196571910	0.0759	0.0157	0.0713	0.0232
Hydruga	*leptonyx*	?	?	K7864	−0.0067	0.0961	−0.0760	−0.0555
Hydruga	*leptonyx*	F	Adult	19404641	−0.0096	0.0837	−0.0813	−0.0459
Hydruga	*leptonyx*	M	Adult	19011415	−0.0087	0.0850	−0.0731	−0.0423
Leptonychotes	*weddelli*	?	?	K7881	0.0387	0.0516	0.0491	−0.0316
Leptonychotes	*weddelli*	?	?	K7884	0.0330	0.0249	0.0541	−0.0202
Leptonychotes	*weddelli*	F	Adult	194046140	0.0359	0.0637	0.0378	−0.0408
Leptonychotes	*weddelli*	F	Adult	194046104	0.0352	0.0331	0.0214	−0.0364
Leptonychotes	*weddelli*	M	Adult	K7883	0.0377	0.0454	0.0115	−0.0388
Leptonychotes	*weddelli*	M	Young	19515111	0.0266	0.0281	0.0599	−0.0285
Lobodon	*carcinophaga*	?	?	K7903	0.0218	0.0405	−0.0543	−0.0577
Lobodon	*carcinophaga*	?	Foetus	19586185	0.0104	−0.0041	−0.0030	−0.0589
Lobodon	*carcinophaga*	M	Adult	19353291	0.0315	0.0251	−0.0800	−0.0589
Lobodon	*carcinophagus*	F	Adult	19404613	0.0262	0.0060	−0.0654	−0.0478
Lobodon	*carcinophagus*	F	Young	184641519	0.0138	0.0214	−0.0045	−0.0614
Lobodon	*carcinophagus*	F	Adult	19591289	0.0233	0.0286	−0.0583	−0.0554
Lobodon	*carcinophagus*	M	Young	184641520	0.0099	0.0438	−0.0346	−0.0668
Lobodon	*carcinophagus*	M	Adult	19591282	0.0452	0.0161	−0.0659	−0.0645
Mirounga	*angustirostris*	F	Young	196610243	0.0486	−0.0213	0.0304	−0.0346
Mirounga	*leonina*	?	Young	193812320	0.0780	−0.0441	0.0638	−0.0575

Mirounga	*leonina*	F	Adult	19517175	0.0533	−0.0016	−0.0201	−0.0538
Mirounga	*leonina*	F	Subadult	19143162	0.0736	−0.0137	0.0257	−0.0542
Mirounga	*leonina*	M	Adult	19395201	0.0838	−0.0559	−0.0888	−0.0702
Mirounga	*leonina*	M	Young	195452038	0.0752	−0.0438	0.0718	−0.0433
Monachus	*monachus*	?	?	K7781	0.0068	0.0233	−0.0132	−0.0080
Monachus	*monachus*	?	Young	18921171	0.0206	−0.0204	0.0416	−0.0016
Monachus	*monachus*	?	Young	18921171	0.0206	−0.0204	0.0416	−0.0016
Monachus	*monachus*	F	Adult	18947272	0.0397	0.0135	−0.0181	0.0005
Monachus	*monachus*	M	Adult	1863411	0.0391	0.0051	−0.0205	−0.0123
Monachus	*schauinslandi*	M	Young	195811261	0.0288	0.0288	0.0060	0.0102
Neophoca	*cinerea*	M	Adult	01939121122	−0.1100	−0.0073	0.0235	−0.0016
Odobenus	*rosmarus*	?	Young	K7499	−0.0227	−0.1716	0.0147	0.0201
Odobenus	*rosmarus*	?	Young	K7481	−0.0075	−0.2030	−0.0275	0.0213
Odobenus	*rosmarus*	F	Adult	K7501	−0.0080	−0.1977	−0.0573	−0.0021
Odobenus	*rosmarus*	F	Foetus	K7503	−0.0744	−0.1660	0.1332	−0.0306
Odobenus	*rosmarus*	F	Young	K7490	0.0068	−0.1540	0.0691	−0.0127
Odobenus	*rosmarus*	M	Adult	K7495	−0.0090	−0.1626	−0.0399	0.0174
Odobenus	*rosmarus*	M	Adult	K7483	0.0109	−0.2095	−0.0451	−0.0019
Ommatophoca	*rossi*	M	Adult	19612243	0.0666	0.0406	0.0107	−0.1071
Ommatophoca	*rossi*	M	Adult	190822049	0.0685	0.0417	0.0216	−0.1098
Otaria	*byronia*	F	Young	0193112118	−0.0942	−0.0133	0.0451	−0.0095
Otaria	*byronia*	F	Adult	01939121190	−0.1193	−0.0036	−0.0427	0.0046
Otaria	*byronia*	M	Young	0195072111	−0.1028	−0.0150	0.0208	−0.0081

Appendix 12.1 (*cont.*)

Genus	Species	Sex	Age	Specimen	PC1	PC2	PC3	PC4
Otaria	*byronia*	M	Young	0193912110	−0.1082	−0.0535	0.0667	−0.0106
Otaria	*byronia*	M	Young	0190822053	−0.1281	−0.0105	0.0279	0.0195
Otaria	*byronia*	M	Adult	019391211168	−0.1007	−0.0547	−0.0594	−0.0166
Otaria	*byronia*	M	Adult	K7030	−0.1038	−0.0680	−0.0734	−0.0168
Phagophilus	*groenlandica*	M	Adult	19637191	0.0438	0.0264	−0.0306	0.0472
Phagophilus	*groenlandica*	M	Young	193811262	0.0450	0.0246	−0.0019	0.0374
Phoca	*groenlandica*	?	Young	18431076	0.0383	0.0082	0.0531	0.0284
Phoca	*hispida*	F	Adult	193710232	0.0411	0.0330	0.0241	0.0337
Phoca	*hispida*	F	Adult	19381264	0.0701	0.0483	0.0155	0.0251
Phoca	*hispida*	M	Young	193710234	0.0602	0.0263	0.0392	0.0313
Phoca	*hispida*	M	Adult	193710231	0.0564	0.0283	0.0194	0.0325
Phoca	*hispida*	M	Young	193710234	0.0602	0.0263	0.0392	0.0313
Phoca	*largha*	F	Adult	196571912	0.0597	0.0412	−0.0068	0.0175
Phoca	*largha*	F	Adult	19657191I	0.0495	0.0453	−0.0250	0.0290
Phoca	*largha*	F	Subadult	196571915	0.0494	0.0496	−0.0053	0.0207
Phoca	*largha*	M	Adult	196571913	0.0305	0.0290	−0.0338	0.0316
Phoca	*vitulina*	?	Young	K8087	0.0484	0.0214	0.0587	0.0147
Phoca	*vitulina*	?	?	K8092	0.0505	0.0086	−0.0257	0.0317
Phoca	*vitulina*	?	?	K80863	0.0447	0.0284	−0.0040	0.0137
Phoca	*vitulina*	?	Young	184632327	0.0282	0.0241	0.0290	−0.0001
Phoca	*vitulina*	M	Adult	184732238	0.0356	0.0244	0.0063	0.0242
Phoca	*vitulina*	?	Young	18863182	0.0386	0.0207	−0.0030	0.0166
Phoca	*vitulina*	?	?	K8173	0.0554	0.0166	−0.0223	0.0218
Phoca	*vitulina*	?	Infant	1004f	0.0324	0.0039	0.0658	0.0118
Phoca	*vitulina*	M	Adult	329i	0.0402	0.0023	−0.0161	0.0237
Pusa	*caspica*	?	?	K8241	0.0634	0.0652	−0.0286	0.0261

Pusa	*caspica*	F	Adult	196371910	0.0488	0.0800	−0.0432	0.0342
Pusa	*caspica*	F	Adult	19657192	0.0434	0.0798	−0.0356	0.0394
Pusa	*caspica*	M	Adult	19657191	0.0434	0.0704	−0.0436	0.0415
Pusa	*caspica*	M	Adult	196371914	0.0584	0.0563	−0.0369	0.0543
Pusa	*hispida*	?	?	K8205	0.0613	0.0308	0.0152	0.0444
Pusa	*hispida*	?	?	K8201	0.0770	0.0248	0.0637	0.0016
Pusa	*sibirica*	F	Adult	19637198	0.0597	0.0447	−0.0068	0.0371
Pusa	*sibirica*	F	Adult	1965961	0.0537	0.0536	−0.0179	0.0381
Pusa	*sibirica*	M	Adult	19637199	0.0645	0.0597	−0.0175	0.0236
Pusa	*sibirica*	M	Young	19657194	0.0524	0.0311	0.0134	0.0326
Pusa	*sibirica*	M	Young	19657193	0.0499	0.0367	0.0169	0.0175
Pusa	*sibirica*	M	Adult	1965962	0.0605	0.0446	−0.0281	0.0401
Zalophus	*californianus*	F	Adult	0190310114	−0.1148	0.0572	−0.0443	0.0172
Zalophus	*californianus*	M	?	K7122m	−0.1021	0.0145	−0.0391	0.0117
Zalophus	*californianus*	M	Young	01898111	−0.1278	0.0267	0.0250	0.0177
Zalophus	*californianus*	M	Young	01952827	−0.1151	0.0467	0.0126	0.0199